



Pre-formed Cooper pairs in copper oxides and LaAlO₃—SrTiO₃ heterostructures

Ivan Božović ^{□ 1,2} and Jeremy Levy ^{□ 3,4} [□]

The Bardeen-Cooper-Schrieffer theory of superconductivity and the Landau-Fermi liquid theory form the basis of our current understanding of conventional superconductors and their parent non-superconducting phases. However, some exotic superconductors do not conform to this physical picture but instead feature an unusual 'normal' state that is not a Fermi liquid. One explanation of this unusual behaviour is that pre-formed pairs of electrons are established above the superconducting temperature T. Here, we highlight recent experiments that show the likely existence of these pre-formed pairs in two rather different materials—a high-temperature cuprate superconductor and strontium titanate. Moreover, in both materials the normal state from which superconductivity emerges has other shared properties, including a pseudogap and electronic nematicity rotational symmetry breaking in the electron fluid that is not expected in Fermi liquid theory nor more generally from the crystal lattice symmetry. These experimental findings should provoke more interaction between the communities working on these materials and new insights into the underlying mechanism of the creation of pre-formed pairs.

early a century ago, Einstein predicted that at sufficiently low temperature, an ideal gas of non-interacting bosons will condense into an unusual quantum form of matter, now known as the Bose-Einstein condensate (BEC). Half a century later, the BEC phase was first observed in ultra-cold, dilute gases of bosonic atoms such as Rb and Na that are weakly interacting and behave like a nearly-ideal Bose gas. Speculations that superconductivity may be due to electron pairs that form below some temperature T_p , and at even lower temperature T_c undergo BEC, also have a long history. However, Bardeen, Cooper, and Schrieffer (BCS) proposed an elegant alternative theory, in which electron pairing and condensation occur simultaneously at T_c . In the BCS model, these Cooper pairs are very large so they overlap significantly and act collectively, essentially the opposite case to a BEC. BCS theory soon became the standard textbook explanation of superconductivity.

The phenomenal success of BCS theory notwithstanding, theorists wondered what would happen if the interaction that glues the electron pairs together increased arbitrarily. The answer, provided by Eagles, Leggett, Nozieres and Schmitt-Rink, is that, at least within the approximation of mean-field theory, one should expect a smooth crossover²⁻⁶ from BCS to BEC (Fig. 1). These predictions were fully confirmed in experiments with ultracold atomic gases. The initial experiments with BEC condensation took place with bosonic atoms^{7,8}. Further refinement in the trapping and cooling of gases of fermionic atoms, combined with the ability to tune the sign and strength of interactions over a wide range, enabled a detailed exploration of the predicted BCS-BEC crossover. Notably, when the pairing interaction in a gas of fermionic atoms is weak, the typical BCS behaviour is seen; when the interaction is boosted, the pair size shrinks until local pre-formed pairs (which, in this case are diatomic molecules) exist and then condense into a BEC superfluid at a lower temperature.

The big open question is whether BEC-like superconductivity could occur in a gas of electrons, given that they are many orders of magnitude lighter and faster than atoms. However, evidence for at least the existence of pre-formed pairs well above T_c in some 'extraordinary' superconductors seems to be very strong. In this Perspective, we highlight some recent experiments on SrTiO₃ and La_{2-x}Sr_xCuO₄ (Fig. 2) that provide the most direct evidence for pre-formed pairs.

Pre-formed pairs in copper oxides

In copper oxides, the high T_c , strong pairing (inferred, for example, from the large ratio of the superconducting gap Δ to $k_{\rm B}T_{\rm c}$), and two-dimensional (2D) nature of superconductivity all point a priori to BEC rather than to BCS superconductivity. Indeed, many have postulated that true BEC occurs in copper oxides, in order to explain why T_c is so high¹⁰⁻¹⁶. The BCS-BEC crossover theory was also invoked to account for extraordinary features of the high-T_c superconductors^{5,6}, including notably the 'pseudogap', a partial depletion of the density of states, (although not a full gap) that develops below a temperature $T > T_c$. This pseudogap was observed by a range of techniques in cuprates and subsequently detected in other materials as well, and associated with anomalous transport and other electronic properties.

However, we emphasize that the existence of pre-formed pairs is a necessary but not sufficient condition for BEC, or for BCS-BEC crossover, to occur. Indeed, since Fermi surfaces have been mapped out by angle-resolved photoemission spectroscopy¹⁷ and quantum oscillations experiments, today many believe that in cooper oxides the physics of strongly correlated fermions evolves into the conventional BCS behaviour when the doping moves past the optimal level that generates the highest T_c . This favours a picture in which pairing is relatively strong, pre-formed pairs first appear at $T_p = T > T_c$ phase fluctuations control T_c , but copper oxides are still on the BCS

Patrick Lee proposed¹⁸ that the pseudogap in high- T_c superconductors originates from a pair-density wave19, an unusual form of electron organization in which electrons pair on the same side of the Fermi surface, thus with large total momentum. In this theory, the other observed orders, such as charge-density waves (CDW), are subdominant18,19. Experimentally, various techniques have provided circumstantial evidence that in copper oxides, pre-formed pairs exist well above the apparent T_c . But in the last few years, more direct evidence has accumulated. One signature is the temperature and doping dependence²⁰ of superfluid density, N_s; it decreases linearly with temperature, while T_c scales with $N_{s0} \equiv N_s(T \rightarrow 0)$, which

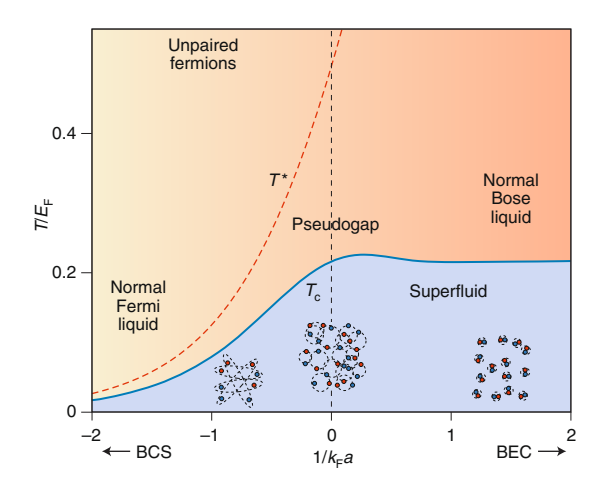


Fig. 1 | Illustration of the phase diagram of the BCS-BEC crossover. Here, T is the pseudogap (or pairing) onset temperature, and T_c is the critical temperature for the onset of superfluidity based on mean-field theory calculations. The horizontal axis is the strength of the coupling, measured by the dimensionless parameter $k_{\rm F}a$, where $k_{\rm F}$ is the Fermi wavevector, and a is the scattering length. Red and blue circles connected by dashed ellipses represent Cooper-paired electrons. In the BCS limit, the pairs overlap strongly, and in the BEC limit they are separated from one another. Figure reproduced with permission from ref. 6 , © Annual Review of Condensed Matter Physics.

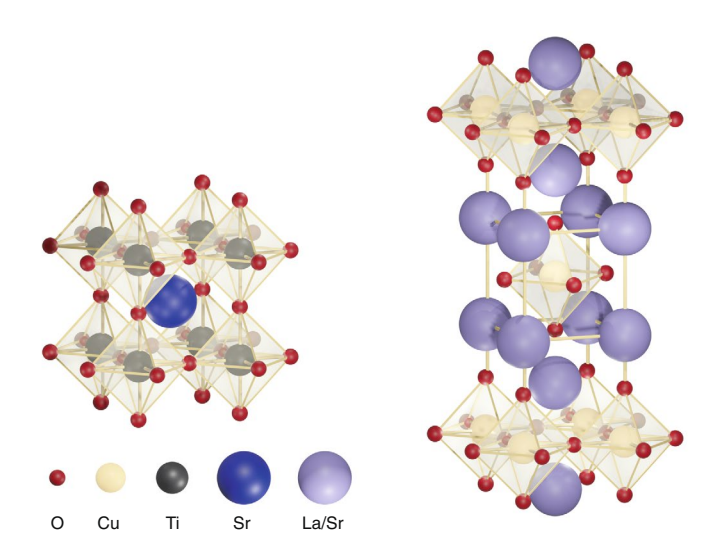


Fig. 2 | Two extraordinary superconductors. $SrTiO_3$ (left) and $La_{2-x}Sr_xCuO_4$ (right). Credit: Yun-Yi Pai

some have associated with BEC. In the standard BCS theory of superconductivity, $T_{\rm c}$ is a complicated function of the electron and phonon dynamics—the electron density of states, the phonon spectrum, and the strength of the electron-phonon interactions. There is no direct relation between $T_{\rm c}$ and $N_{\rm so}$; the latter should be equal to the normal-state electron density. In cuprates, $T_{\rm c}$ is a simple (almost linear) function of $N_{\rm so}$, so that $T_{\rm c}$ is essentially just determined by the kinematics, as in BEC.

Most recently, shot-noise measurements have been reported on $\text{La}_{2-x}\text{Sr}_x\text{CuO}_4$ -based tunnel junctions²¹. 'Shot noise' is a moniker for current fluctuations that originate from the discrete nature of the charge carriers. The intensity of the shot noise, S_1 , is related to the charge q of the mobile carriers as $S_1 = 2qI \, \text{coth}[qV/(2k_BT)]$, where T is the temperature, I is the probe current and V is the bias

voltage. Hence, by measuring S_1 as a function of T and V, one can directly read the T- and V- dependence of the effective charge. In ref. 21 , it was indeed found that in the normal state—meaning at high enough T and V—the effective charge q equals the electron charge e. However, q > e in a large portion of the V - T phase diagram outside of the superconducting gap region. As a minimal model, one can assume that a fraction f of the electrons is paired, and read f from the measured q. The data are presented in Fig. 3 as f(T, V). Evidently, pairs exist in at least a large portion of the V - T phase diagram attributed to the pseudogap²¹ (Fig. 3).

But we emphasize that the simple BEC picture also disagrees with a range of experimental findings. For example, recent terahertz experiments indicated²² that the electron fluid seems to behave more like a two-component (fermion and boson) mixture, in which the bosonic component controls T_c , but decreases and disappears with overdoping.

It is also fair to mention that there are alternative views about the pseudogap state in the cuprates that do not require pre-formed pairs, such as a competing order or magnetic precursors. However, the shot-noise experiments (ref. ²¹) show that this cannot be the whole story—pre-formed pairs are seen, directly, in at least a large portion of the phase diagram occupied by the pseudogap state.

Pre-formed pairs in SrTiO₃

SrTiO₃ was the first example of a superconducting semiconductor and the first to show a superconducting dome, and has long been suspected to harbour pre-formed electron pairs^{23,24}. Interest in the superconducting properties of SrTiO₃ was reignited with the discovery of emergent conductivity at the LaAlO₃/SrTiO₃ interface²⁵, which inherits most of its properties from bulk SrTiO₃.

Key features of the LaAlO₃/SrTiO₃ system include the 2D nature of the superconducting state²⁶, and the ability to tune through the superconducting dome by applying a perpendicular electric field²⁷. Apart from the high k_BT_c/E_F ratio²⁸ (measured for bulk SrTiO₃) and the superconducting dome, another similarity with the copper-oxides was identified by Richter et al.²⁹ who used tunnelling experiments to find a pseudogap phase that persisted up to $T \approx 500$ mK, above the maximum observed $T_c \approx 300$ mK.

Direct evidence for pre-formed pairs came from experiments by Cheng et al.30 on single-electron transistors (SETs) created at the LaAlO₃/SrTiO₃ interface (Fig. 4a). SET measurements are able to 'count' electrons as they accumulate on a small quantum dot by measuring resonant tunnelling on and off the dot. Peaks in tunnelling current through the SET allow the charge on the quantum dot to be directly counted. Classic parity measurements from Tinkham's group³¹ on superconducting aluminium SETs showed how the 2e charging periodicity of the superconducting quantum dot disappears at $T \approx 300$ mK, below the bulk $T_c = 1.2$ K transition temperature. In contrast, the experiments of Cheng et al.30 show even-parity charging (meaning that the charge on the dot jumps by two in a sequence like 2(N-1)e, 2Ne, 2(N+1)e) of the LaAlO₃/SrTiO₃ dot at temperatures T > 900 mK $\approx 3T_c$. Above a critical pairing field $B_p=2T$ (Fig. 4b), charging alternates between even and odd parity (like 2(N-1)e, (2N-1)e, 2Ne, 2(N+1)e), as indicated by the dashed line near B = 4T in Fig. 4b. The pairing field exceeds the known upper critical field ($B_{c2} \sim 0.2$ T) for superconductivity in SrTiO₃ by an order of magnitude. The system exhibits three distinct phases: superconducting ($|B| < B_{c2}$, paired and non-superconducting $(B_{c2} < |B| < B_p)$, and normal $(|B| > B_p)$. At higher magnetic fields, re-entrant pairing can occur, for example, the transition between (2N-1)e and (2N+1)e charge states in Fig. 4b.

A separate set of experiments shows that pairing without superconductivity can exist not only in quantum dots, but quantum wires as well. Annadi et al. observed quantized ballistic transport in LaAlO₃/SrTiO₃-based electron waveguides³². In the ballistic limit, conductance G is expected to be quantized: $G = Ne^2/h$, where N

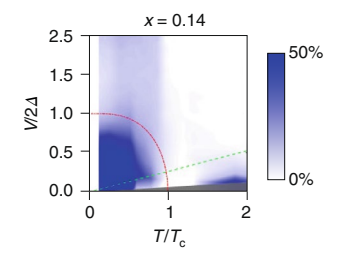


Fig. 3 | Proportion of tunnelling pairs inferred from shot-noise measurements. The data are taken for $La_{2-x}Sr_xCuO_4/LaCuO_4/La_{2-x}Sr_xCuO_4$ tunnel junctions for doping x=0.14. Red dash-dotted lines show the superconducting gap region, outside which there should be no pairs according to BCS theory. Green dashed line shows $V=k_BT/e$. Data are inconclusive in the grey area. Figure reproduced with permission from ref. 21 , Springer Nature Ltd.

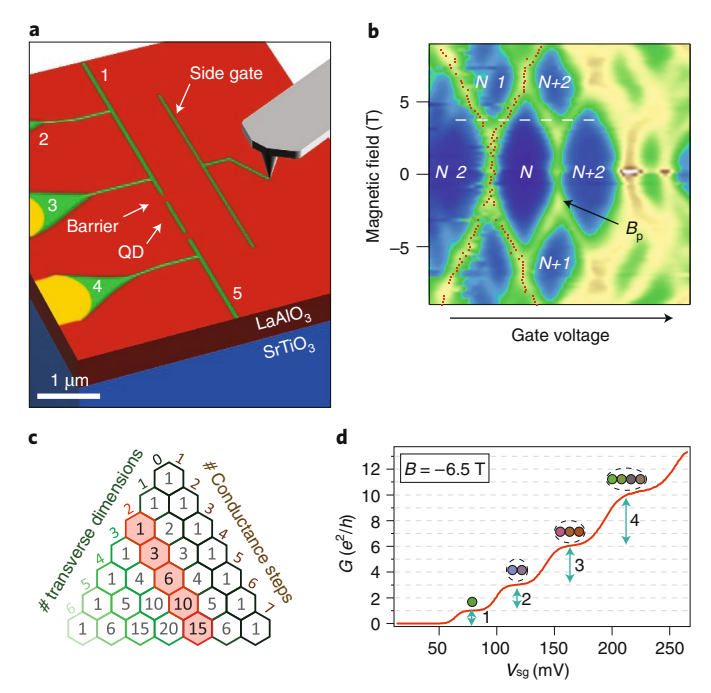


Fig. 4 | Pre-formed electron pairs and their generalizations in LaAlO₃/ **SrTiO**₃ **nanowires. a**, Illustration of a single-electron transistor (SET) used to observe pre-formed pairs. **b**, Conductance of SET as a function of magnetic field and gate voltage. Stable regions (dark blue) of low conductance are separated by (green) peaks that bifurcate at $B_p = 2$ T. Dashed line shows SET charging with e-periodicity. **c**, Pascal's triangle helps describe quantized conduction of LaAlO₃/SrTiO₃ electron waveguides. The shaded diagonal denotes a family of composite electronic states with two transverse degrees of freedom. **d**, Quantized conductance steps associated with a series of degenerate quantum liquids composed of charge-*ne* particles, where n = 1, 2, 3, 4, ..., N, and total conductance $G = N(N+1)e^2/h$. Figure adapted with permission from: **a,b**, ref. ³⁰, Springer Nature Ltd; **c,d**, ref. ⁵⁷, AAAS.

counts the total number of quantum channels (which are distinguished by transverse degrees of freedom and spin). At sufficiently low magnetic fields, electron sub-bands can 'lock' together and form pair liquids (due to the same attraction that gives rise to superconductivity). The quantization of conductance then takes place in steps of $2e^2/h$ due to the ballistic pair transport. This state is stable up to a pairing field that matches values found in the SET experiments described earlier. When certain conditions are satisfied, it is

possible for more than two sub-bands to intersect and lock together. Figure 4c shows how Pascal's triangle can help organize the degeneracies that give rise to the sequence of conductance plateaus at $(1, 3, 6, 10, \ldots)e^2/h$ observed in a LaAlO₃/SrTiO₃ quantum wire (Fig. 4d), where V_{sg} is the side-gate voltage of the SET. The interpretation of this phase is that electrons are forming bound particles with $n=2, 3, 4, 5, \ldots$ electrons, which form degenerate quantum liquids. This remarkable phase can be regarded as a generalization of pre-formed pairs, and an example of the emergent complexity that can be found in 1D quantum systems with attractive electronelectron interactions.

Comparative case study of electronic nematicity

SrTiO₃ and the copper oxides have many features that distinguish them from one another. T_c differs by orders of magnitude, the pairing symmetry is quite different (d-wave for copper oxides, and most likely s-wave for SrTiO₃), and the parent insulating phase is fundamentally different (Mott insulator for copper oxides and a band insulator for SrTiO₃). Despite the differences, it is worth examining some of the striking similarities between these two systems. Apart from the existence of a superconducting dome, the systems also exhibit a pseudogap phase and show direct evidence for pre-formed pairs. In both cuprates and SrTiO₃ the superfluid density is unusually low; the pairs are 'dilute' and hardly overlap at all. The numberphase uncertainty relation thus mandates that there must be a broad regime of phase fluctuations, quantum or thermal. This leads to the existence of pre-formed pairs well above T_c . Note that this is qualitatively new physics, different from the standard textbook description of superconductivity based on a mean-field (BCS) theory. Here, T_c is controlled by the loss of phase coherence, while incoherent pairs survive to much higher temperature.

In fact, there are more similarities worth examining. As a 'case study', here we compare reports of electronic nematicity in the $\text{La}_{2-x}\text{Sr}_x\text{CuO}_4$ with what we argue to be similar behavior in $\text{LaAlO}_3/\text{SrTiO}_3$ systems. The motivation for including it here is that the pseudogap, pre-formed pairs and nematicity are most likely related to one another, although the exact relation is not clear yet. Theoretically, the simplest scenario would be that all these are just different manifestations of one and the same state. For example, it has been proposed that in cuprates all these originate from an incipient pair density wave order 14. More generally, pre-formed pairs look like the most natural candidate for electronic 'nematogens'. Experimentally, in both cuprates and SrTiO_3 the pseudogap, pre-formed pairs and nematicity clearly coexist and overlap in much of the phase diagram, but it is still an open question whether they exactly coincide.

It has long been recognized that the under-doped regime could be unstable to broken symmetries not obvious from the underlying structure. In addition to efforts to elucidate the nature of the pseudogap phase, investigations of electronic nematicity^{33,34} have attracted the attention in both theory and experiment. Wu et al.35 fabricated radially aligned Hall bars (Fig. 5a,b) in La2-xSrxCuO4 and studied the dependence of longitudinal and transverse resistivity (Fig. 5c) on in-plane orientation, temperature and doping. In Fig. 5c, the measured transverse resistivity $\rho_{\rm T}(\phi)$ is plotted in polar coordinates, where the radial distance measures the magnitude of $\rho_{T}(\phi)$, with the positive values shaded in blue and negative in red, while the polar angle ϕ corresponds to the current direction. The lowest resistivity direction is along the diagonal with red to the right and blue to the left. The phase diagram in Fig. 5d shows the nematicity amplitude $N = (\rho_a - \rho_b)/(\rho_a + \rho_b)$, where ρ_a and ρ_b are the maximal and minimal resistivities, respectively, as a function of T and the doping level p. The clover-shaped anisotropy, as seen in Fig. 5c (and not to be confused with the d-wave superconducting order parameter), was found to be largest at low doping, decreasing significantly and monotonically with increased doping, and persisting

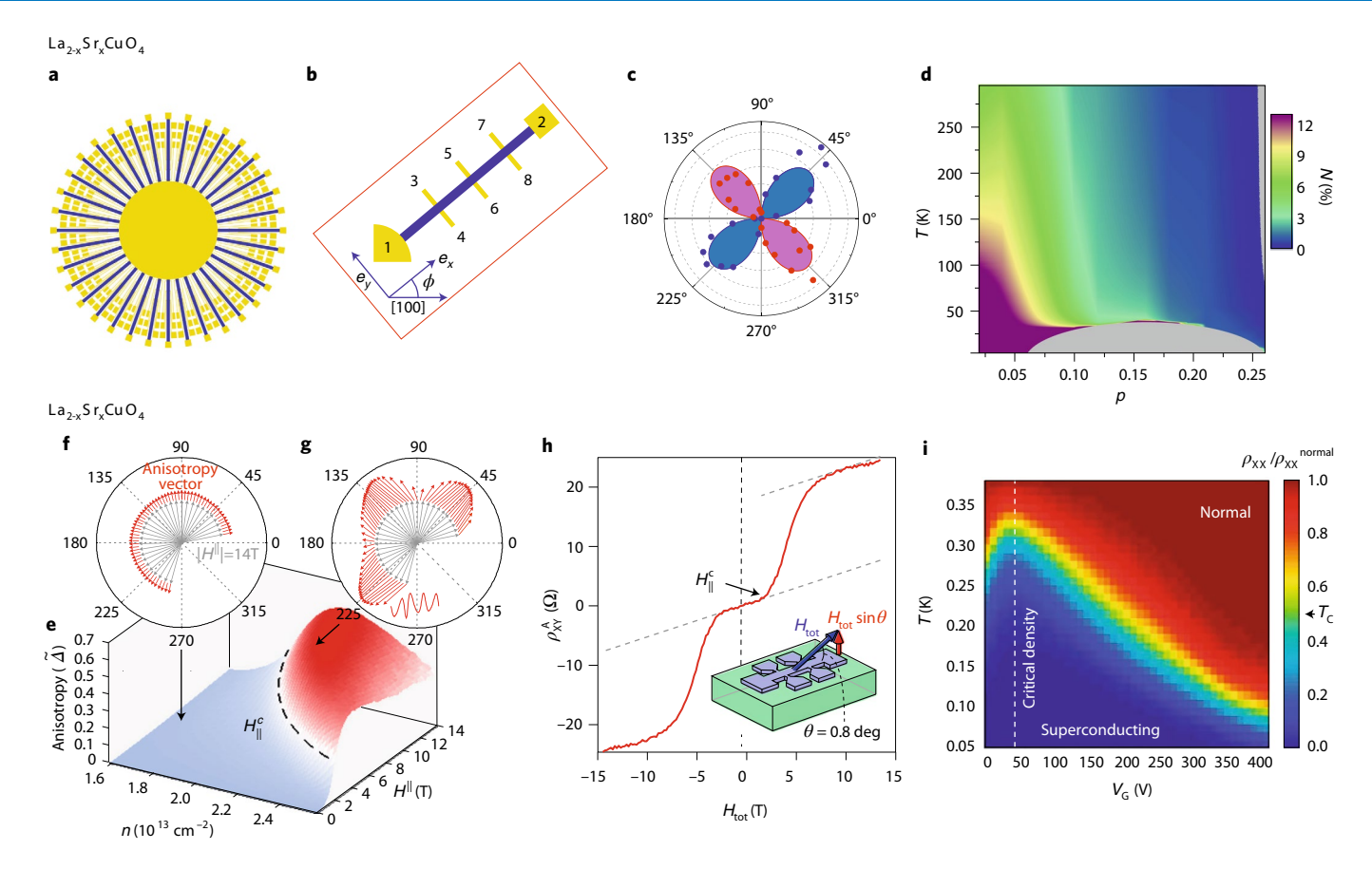


Fig. 5 | Comparison of electronic nematicity in La_{2-x}Sr_xCuO₄ and LaAlO₃/SrTiO₃. **a**, Radial array of La_{2-x}Sr_xCuO₄ Hall bars. **b**, A single Hall bar, oriented at angle ϕ with respect to the [100] direction. e_x and e_y , unit vectors along the x and y axes, respectively. **c**, Polar plot of transverse resistivity versus ϕ , a key signature of electronic nematicity. Blue and red colours denote positive and negative values, respectively. **d**, Map of nematicity strength N versus temperature T and doping p. **e**, Map of magnetoresistance anisotropy of LaAlO₃/SrTiO₃ as a function of carrier density n and in-plane magnetic field H^{\parallel} . A clear phase boundary (dashed line $H^c_{\parallel}(n)$) separates an isotropic phase (blue, **f**) and anisotropic phase (red, **g**). **h**, Anomalous Hall effect onset begins at H^c_{\parallel} , coinciding with the nematic phase boundary. H_{tot} total magnitude of the applied magnetic field; ρ_{Xy}^A , antisymmetrized Hall resistance. **i**. Phase diagram indicating that the peak of the superconducting dome exists at the critical density n_c at which the critical field H^c_{\parallel} diverges. $\rho_{\text{XX}}/\rho_{\text{XX}}^{\text{normal}}$, longitudinal resistance normalized to its value in the normal state; V_G , gate voltage. Figure adapted with permission from: **a**-**d**, ref. ³⁵, Springer Nature Ltd; **e**-**h**, ref. ³⁸, PNAS; **i**, ref. ³⁹, Springer Nature Ltd.

all the way to room temperature, outside of the pseudogap regime. However, it did not change when a large unidirectional in-plane strain was applied; moreover, the lowest-resistivity direction was found to vary strongly with both temperature and doping. These findings seem to rule out direct crystalline origins.

Unusual anisotropy of in-plane magnetoresistance at the LaAlO₃/SrTiO₃ interface was first reported by Ben Shalom et al.³⁶, and later by Fête et al.37, but the most thorough experimental investigation came from Joshua et al.38. They measured the magnetoresistance of a fixed Hall bar (aligned along a crystallographic axis) as a function of a symmetry-breaking in-plane magnetic field (of varying magnitude and direction) and the carrier density (which is controlled by back-gate tuning) and found an unusual phase diagram: at sufficiently weak in-plane magnetic field, the induced anisotropic response follows the field direction (Fig. 5h). Above a critical density $n_c \approx 1.6 \times 10^{13} \text{cm}^{-2}$ and above a critical magnetic field that depends on the density $H_{\parallel}^{c}(n)$, there is a sharp transition to a phase in which the magnetic anisotropy magnitude increases significantly, and ceases to follow the applied magnetic field but instead tends to favour (approximately) the $\pm 45^{\circ}$ and $\pm 135^{\circ}$ diagonals. The same boundary also is associated with the onset of an anomalous Hall effect (Fig. 5h). The phase boundary $H_{\parallel}^{c}(n)$ can be as small as 2 T far above n_c , and nearly diverges near n_c . The critical density, previously identified³⁹ with a Lifshitz transition introducing d_{xz} and d_{yz} bands, coincides with the peak of the superconducting dome (Fig. 5i). This unusual phase diagram and the anomalous Hall offset may be connected with the pairing transition⁴⁰, and linked to electron–electron interactions and correlation effects at the Lifshitz transition^{41–44}. Subsequent measurements involving local probes have revealed that the anisotropic transport is associated with current that flows preferentially along ferroelastic domain boundaries whose orientation does not respect the crystalline axes. Evidence for inhomogeneous transport is covered in a recent review article by Pai et al.⁴⁵. Although these experimental results are not described by the authors in terms of nematicity, it is our perspective that the data meets the criteria for electronic nematicity, in that the in-plane anisotropy disappears below a critical magnetic field, and does not precisely coincide with the crystallographic directions.

Apart from electronic nematicity, other shared characteristics seem worthy of further scrutiny. For example, stripe phases exist in LaAlO₃/SrTiO₃ that appear to play a defining role in the superconducting state. These spontaneously occurring ferroelastic domains form 1D boundaries at the 2D LaAlO₃/SrTiO₃ interface, and there is evidence from scanning probes^{46,47} and artificially defined structures³² that these stripe edges support ballistic conduction and 1D superconductivity, and may play a functional role in the pairing 'glue'^{48,49}. Theories initially developed for the copper oxides, for

example ref. 50 , may find relevance for the pairing and superconductivity phenomena in SrTiO $_3$.

Outlook

Careful examination of the similarities between these two extraordinary families of superconductors, despite their obvious differences, may yet reveal useful insights. While LaAlO₃/SrTiO₃ is clearly distinct from bulk SrTiO₃, lessons learned about LaAlO₃/SrTiO₃ should ultimately be transferrable to the 3D system. Put alternatively, it is unlikely that the pairing mechanism for LaAlO₃/SrTiO₃ and SrTiO₃ are entirely distinct. Understanding how the LaAlO₃/SrTiO₃ system superconducts with so few electrons may deepen our understanding of exotic superconductivity more generally, and perhaps guide discovery of new superconductors. The LaAlO₃/SrTiO₃ system is much simpler than its higher-temperature relatives, and has the advantages of gate tunability²⁷, 'programmability' at extreme nanoscale dimensions⁵¹ and direct access to the paired liquid state.

Shot-noise experiments on $La_{2-x}Sr_xCuO_4$ could be expanded to include systematic study of varying the barrier transparency, the entire doping range, and different insulators as the barrier material. Then one should probe other copper oxides, including all the key families (YBa₂Cu₃O_{7-x}, Bi-, Hg- and Ti-based copper oxides, and electron-doped ones). An obvious question is whether the shot-noise phenomena observed in $La_{2-x}Sr_xCuO_4$ are indeed generic to all copper-oxide superconductors, or perhaps just an anomaly specific to this material.

Recent work on strain-engineered SrTiO₃ shows that T_c can be more than doubled (to $T_c = 670$ mK) by growing on lattice-mismatched substrates⁵². In addition, narrow SrTiO₃ quantum wells have been found to exhibit large ($\Delta = 33$ meV) pseudogap features⁵³. This motivates exploration of possible links between this pseudogap and pairing at room temperature, and of ways to enhance coherence between pairs and increase T_c further.

Looking beyond copper oxides and SrTiO₃, it is worth examining what other candidate materials could host superconductivity, pseudogaps and pre-formed pairs. In recent years, pseudogap features have been identified in several dozen materials. We can tentatively divide these reports into three classes, as follows.

- Superconductors in which the pseudogap has been attributed to superconducting fluctuations. Examples include amorphous InO, disordered NbN, 1T-TiSe₂, and so on, in which, presumably, disorder triggers Anderson localization that competes with phonon-mediated BCS-type superconductivity^{54,55}. These are discussed extensively in the accompanying Review by Sacépé et al. in ref. ⁵⁶. Another example is FeSe, but it may be more akin to cuprates, with electron correlations, nematicity, antiferromagnetic fluctuations playing a role.
- 2. Superconductors in which the pseudogap has been attributed to a competing charge or spin order (such as charge- or spin-density waves). Notable examples include a heavy fermion superconductor CeCoIn₅ and quasi-2D superconductors LiHfNCl and LiZrNCl. Some FeAs-based superconductors, as well as FeTe_{1-x}Se_x, have been proposed to be in this category.
- 3. Materials that show a pseudogap but (so far) no superconductivity. In recent years, many examples have been discovered, including binary oxides such as NbO₂, hexagonal e-TiO and h-TiO, electron-doped oxides with perovskite structure such as (Nd,Sr)VO₃, 214 structure (SrIrO₄), or 327 structure (Sr₃Ru₂O₇, Ca₃Ru₂O₇), as well as intermetallic compounds like SmB₆ and t-PtGa₂.

It would be revealing and rewarding to explore all of these, probing for the existence of pre-formed pairs directly through shot noise or mesoscopic transport techniques. In the case of point 1, above, one certainly expects to see pre-formed pairs above T_c , in the region of superconducting fluctuations. The big question here is whether

they will be also observed outside and beyond that region, as in $La_{2-x}Sr_xCuO_4$.

Another important question is whether inhomogeneity plays a key role also in $La_{2-x}Sr_xCuO_4$, as surmised by Kresin et al. ⁵⁴, among others. In the case of point 2, above, the theory suggests that one would not expect to see pre-formed pairs, but this should be checked.

Perhaps the most potentially interesting discoveries may loom within the group of point 3, above. While in most of these materials it is probably charge- or spin-density waves that partially gap the Fermi surface, it is not inconceivable that in some cases the observed pseudogap in fact originates from electron pairing. Materials with large pairing gaps (but no observable superconductivity) might be manipulated to induce or increase phase coherence and achieve superconductivity at record-high temperatures.

Received: 7 September 2019; Accepted: 21 April 2020; Published online: 7 July 2020

References

- Bardeen, J., Cooper, L. N. & Schrieffer, J. R. Theory of Superconductivity. *Phys. Rev.* 108, 1175–1204 (1957).
- Eagles, D. M. Possible pairing without superconductivity at low carrier concentrations in bulk and thin-film superconducting semiconductors. *Phys. Rev.* 186, 456–463 (1969).
- 3. Leggett, A. J. Diatomic molecules and cooper pairs (Springer, 1980).
- Nozières, P. & Schmitt-Rink, S. Bose condensation in an attractive fermion gas: from weak to strong coupling superconductivity. J. Low Temp. Phys. 59, 195–211 (1985).
- Chen, Q., Stajic, J., Tan, S. & Levin, K. BCS-BEC crossover: from high temperature superconductors to ultracold superfluids. *Phys. Rep.* 412, 1–88 (2005).
- Randeria, M. & Taylor, E. Crossover from Bardeen-Cooper-Schrieffer to Bose-Einstein Condensation and the Unitary Fermi Gas. Ann. Rev. Cond. Matt. Phys. 5, 209–232 (2014).
- Cornell, E. A. & Wieman, C. E. Nobel lecture: Bose-Einstein condensation in a dilute gas, the first 70 years and some recent experiments. *Rev. Mod. Phys.* 74, 875–893 (2002).
- Ketterle, W. Nobel lecture: When atoms behave as waves: Bose-Einstein condensation and the atom laser. Rev. Mod. Phys. 74, 1131–1151 (2002).
- Greiner, M., Regal, C. A. & Jin, D. S. Emergence of a molecular Bose– Einstein condensate from a Fermi gas. *Nature* 426, 537–540 (2003).
- Anderson, P. W. The theory of superconductivity in the high-T_c cuprates (Princeton Univ. Press, 1997).
- 11. Friedberg, R. & Lee, T. D. Boson-Fermion model of superconductivity. *Phy. Lett. A* 138, 423–427 (1989).
- Alexandrov, A. S. & Mott, N. F. High Temperature Superconductors and Other Superfluids (Taylor & Francis, 1994).
- Zhao, G.-m, Hunt, M. B., Keller, H. & Müller, K. A. Evidence for polaronic supercarriers in the copper oxide superconductors La_{2-x}Sr_xCuO₄. *Nature* 385, 236–239 (1997).
- Deutscher, G. & de Gennes, P.-G. A spatial interpretation of emerging superconductivity in lightly doped cuprates. *Comp. Rend. Phys.* 8, 937–941 (2007).
- Andreev, A. F. Electron pairs for HTSC. J. Exp. Theor. Phys. Lett. 79, 88–90 (2004).
- Jiang, S., Zou, L. & Ku, W. Non-Fermi-liquid scattering against an emergent Bose liquid: manifestations in the kink and other exotic quasiparticle behavior in the normal-state cuprate superconductors. *Phys. Rev. B* 99, 104507 (2019).
- Damascelli, A., Hussain, Z. & Shen, Z.-X. Angle-resolved photoemission studies of the cuprate superconductors. Rev. Mod. Phys. 75, 473–541 (2003).
- 18. Lee, P. A. Amperean pairing and the pseudogap phase of cuprate superconductors. *Phys. Rev. X* **4**, 031017 (2014).
- 19. Hamidian, M. H. et al. Detection of a Cooper-pair density wave in $Bi_2Sr_2CaCu_2O_{8+x}$. Nature **532**, 343–347 (2016).
- Božović, I., He, X., Wu, J. & Bollinger, A. T. Dependence of the critical temperature in overdoped copper oxides on superfluid density. *Nature* 536, 309–311 (2016).
- Zhou, P. et al. Electron pairing in the pseudogap state revealed by shot noise in copper-oxide junctions. *Nature* 572, 493–496 (2019).
- Mahmood, F., He, X., Božović, I. & Armitage, N. P. Locating the missing superconducting electrons in the overdoped cuprates La_{2.x}Sr_xCuO₄. Phys. Rev. Lett. 122, 027003 (2019).
- 23. Schooley, J. F., Hosler, W. R. & Cohen, M. L. Superconductivity in semiconducting SrTiO₃. *Phys. Rev. Lett.* **12**, 474–475 (1964).

- Koonce, C. S., Cohen, M. L., Schooley, J. F., Hosler, W. R. & Pfeiffer, E. R. Superconducting transition temperatures of semiconducting SrTiO₃. *Phys. Rev.* 163, 380–390 (1967).
- Muller, D. A., Nakagawa, N., Ohtomo, A., Grazul, J. L. & Hwang, H. Y. Atomic-scale imaging of nanoengineered oxygen vacancy profiles in SrTiO3. Nature 430, 657–661 (2004).
- Reyren, N. et al. Superconducting interfaces between insulating oxides. Science 317, 1196–1199 (2007).
- Caviglia, A. D. et al. Electric field control of the LaAlO₃/SrTiO₃ interface ground state. *Nature* 456, 624–627 (2008).
- 28. Lin, X., Zhu, Z., Fauqué, B. & Behnia, K. Fermi surface of the most dilute superconductor. *Phys. Rev. X* **3**, 021002 (2013).
- Richter, C. et al. Interface superconductor with gap behaviour like a high-temperature superconductor. *Nature* 502, 528–531 (2013).
- 30. Cheng, G. et al. Electron pairing without superconductivity. *Nature* **521**, 196–199 (2015).
- 31. Tuominen, M. T., Hergenrother, J. M., Tighe, T. S. & Tinkham, M. Experimental evidence for parity-based 2e periodicity in a superconducting single-electron Tunneling Transistor. *Phys. Rev. Lett.* **69**, 1997–2000 (1992).
- 32. Annadi, A. et al. Quantized ballistic transport of electrons and electron pairs in LaAlO₃/SrTiO₃ Nanowires. *Nano Lett.* **18**, 4473–4481 (2018).
- Kivelson, S. A., Fradkin, E. & Emery, V. J. Electronic liquid-crystal phases of a doped Mott insulator. *Nature* 393, 550–553 (1998).
- Fradkin, E., Kivelson, S. A., Lawler, M. J., Eisenstein, J. P. & Mackenzie, A. P. Nematic Fermi Fluids in Condensed Matter Physics. *Ann. Rev. Cond. Matt. Phys.* 1, 153–178 (2010).
- 35. Wu, J., Bollinger, A. T., He, X. & Božović, I. Spontaneous breaking of rotational symmetry in copper oxide superconductors. *Nature* **547**, 432–435 (2017).
- Ben Shalom, M. et al. Anisotropic magnetotransport at the SrTiO₃/LaAlO₃ interface. *Phys. Rev. B* 80, 140403 (2009).
- Fête, A., Gariglio, S., Caviglia, A. D., Triscone, J. M. & Gabay, M. Rashba induced magnetoconductance oscillations in the LaAlO₃-SrTiO₃ heterostructure. *Phys. Rev. B* 86, 201105 (2012).
- 38. Joshua, A., Ruhman, J., Pecker, S., Altman, E. & Ilani, S. Gate-tunable polarized phase of two-dimensional electrons at the LaAlO₃/SrTiO₃ interface. *Proc. Natl Acad. Sci. USA* **110**, 9633 (2013).
- Joshua, A., Pecker, S., Ruhman, J., Altman, E. & Ilani, S. A universal critical density underlying the physics of electrons at the LaAlO₃/SrTiO₃ interface. *Nat. Commun.* 3, 1129 (2012).
- 40. Pai, Y.-Y., Tylan-Tyler, A., Irvin, P. & Levy, J. in Spintronics Handbook 2nd edn, Vol. 2 (CRC, 2019).
- Maniv, E. et al. Strong correlations elucidate the electronic structure and phase diagram of LaAlO₃/SrTiO₃ interface. Nat. Commun. 6, 8239 (2015).
- Cheng, G. et al. Tunable electron-electron interactions in LaAlO₃/SrTiO₃ nanostructures. *Phys. Rev. X* 6, 041042 (2016).
- Smink, A. E. M. et al. Gate-tunable band structure of the LaAlO₃/SrTiO₃ Interface. *Phys. Rev. Lett.* 118, 106401 (2017).
- Trevisan, T. V., Schütt, M. & Fernandes, R. M. Unconventional multiband superconductivity in bulk SrTiO₃ and LaAlO₃/SrTiO₃ interfaces. *Phys. Rev. Lett.* 121, 127002 (2018).
- Pai, Y.-Y., Tylan-Tyler, A., Irvin, P. & Levy, J. Physics of SrTiO₃-based heterostructures and nanostructures: a review. *Rep. Prog. Phys.* 81, 036503 (2018).

- 46. Kalisky, B. et al. Locally enhanced conductivity due to the tetragonal domain structure in LaAlO₃/SrTiO₃ heterointerfaces. *Nat. Mater.* 12, 1091–1095 (2013).
- 47. Honig, M. et al. Local electrostatic imaging of striped domain order in LaAlO₃/SrTiO₃. *Nat. Mater.* **12**, 1112–1118 (2013).
- 48. Pai, Y.-Y. et al. One-dimensional nature of superconductivity at the LaAlO₃/SrTiO₃ interface. *Phys. Rev. Lett.* **120**, 147001 (2018).
- Pekker, D., Hellberg, C. S. & Levy, J. Theory of superconductivity at the LaAlO₃/SrTiO₃ heterointerface: electron pairing mediated by deformation of ferroelastic domain walls. Preprint at https://arxiv.org/abs/2002.11744 (2020).
- Emery, V. J., Kivelson, S. A. & Zachar, O. Spin-gap proximity effect mechanism of high-temperature superconductivity. *Phys. Rev. B* 56, 6120–6147 (1997).
- Cen, C. et al. Nanoscale control of an interfacial metal-insulator transition at room temperature. Nat. Mater. 7, 298–302 (2008).
- 52. Ahadi, K. et al. Enhancing superconductivity in SrTiO₃ films with strain. *Sci. Adv.* 5, eaaw0120 (2019).
- Marshall, P. B., Mikheev, E., Raghavan, S. & Stemmer, S. Pseudogaps and emergence of coherence in two-dimensional electron liquids in SrTiO₃. *Phys. Rev. Lett.* 117, 046402 (2016).
- Kresin, V. Z., Ovchinnikov, Y. N. & Wolf, S. A. Inhomogeneous superconductivity and the "pseudogap" state of novel superconductors. *Phys. Rep.* 431, 231–259 (2006).
- Sacépé, B. et al. Localization of preformed Cooper pairs in disordered superconductors. Nat. Phys. 7, 239–244 (2011).
- Sacépé, B., Feigel'man, M. & Klapwijk, T. M. Quantum breakdown of superconductivity in low-dimensional materials. *Nat. Phys.* https://doi. org/10.1038/s41567-020-0905-x (2020).
- Briggeman, M. et al. Pascal conductance series in ballistic one-dimensional LaAlO3/SrTiO3 channels. Science 367, 769–772 (2020).

Acknowledgements

The research at Brookhaven National Laboratory was supported by the US Department of Energy, Basic Energy Sciences, Materials Sciences and Engineering Division. The work at Yale was supported by the Gordon and Betty Moore Foundation's EPiQS Initiative through grant no. GBMF4410. The work at Pittsburgh was supported by a Vannevar Bush Faculty Fellowship program sponsored by the Basic Research Office of the Assistant Secretary of Defense for Research and Engineering and funded by the Office of Naval Research through grant no. N00014-15-1-2847, and NSF grant no. PHY-1913034.

Competing interests

The authors declare no competing interests.

Additional information

Correspondence should be addressed to J.L.

Reprints and permissions information is available at www.nature.com/reprints.

Publisher's note Springer Nature remains neutral with regard to jurisdictional claims in published maps and institutional affiliations.

© Springer Nature Limited 2020